12-1973

Ultrastructure of Inclusion Bodies in the Transitional Epithelium of Monkey Urinary Bladder

Alan B. Weckerling
Incarnate Word College

This Thesis for the Master of Science Degree

by

Alan B. Weckerling

has been approved for the

Division of Graduate Studies of

Incarnate Word College

by

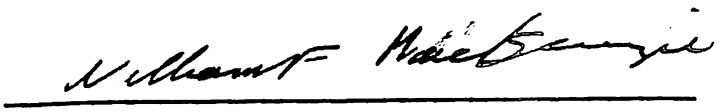

William F. MacKenzie, D.V.M., M.S.

Major Professor

Donald D. McLain, Ph.D.,

Moody Foundation Professor of Biology

Reader

San Antonio, Texas

December, 1973

ULTRASTRUCTURE OF INCLUSION BODIES IN THE TRANSITIONAL EPITHELIUM OF MONKEY URINARY BLADDER

by

Alan B. Weckerling

A Thesis

Submitted to the Faculty of the Division of Graduate Studies of Incarnate Word College in Partial Fulfilment of the Requirements for the Degree of

Master of Science

Department of Biology

San Antonio, Texas

December, 1973

DEDICATION

I would like to dedicate this thesis to my beautiful wife, Sally, without whose help and encouragement this thesis surely would not have been completed.

TABLE OF CONTENTS

This thesis follows the format of The Journal of Cell Biology.

INTRODUCTION

It has been noted that hematoxylin-eosin stained surface cells in the transitional epithelium of certain animals occasionally contain acidophilic inclusion bodies (25). These can be observed in monkey kidney pelvis, ureter, urinary bladder, and urethra (plate 1).

In one species of monkey, Macaca fascicularis, the inclusion bodies are quite prevalent and apparently are not related to any pathologic or experimental condition. They are highly refractile under the light microscope, a property which often indicates structures below the resolving power of the microscope (plate 2).

This study was designed to explore the composition and structure of these inclusion bodies. Procedures were selected to detect the presence of lysosomes, viruses, proteins, lipids, and carbohydrates and these histochemical studies were correlated with electron microscopic examinations. Results of these analyses support the conclusion that these bodies are keratin.

LITERATURE REVIEW

Transitional epithelium is the lining of the excretory passages of the urinary system (31). The locations in which this tissue is found are the kidney pelvis, ureter, urinary bladder and urethra (15). The microscopic appearance of this tissue is described by diFiore (12) and Abdin (2) as consisting of three cell layers capable of stretching to contain the wide variances in the volume of the urine stored in the bladder. The nondistended bladder has a very infolded mucosa. Roberts and Seibold (32) indicated that the transitional epithelium of monkeys is essentially similar to that of man.

The transitional epithelium of the monkey has not been described in detail previously; therefore, a composite description of various other species will be presented. The ultrastructure of the transitional epithelial cells of the mouse is described by both Porter and Bonneville (30) and Fawcett (14) as having a scalloped surface with a layer of fibers under that surface. The cells, which possess a normal complement of organelles in all species reported, are arranged trilaminarly in the mouse according to Walker (44). Richter and Moize (31) made an additional report which broadened Walker's observations. They indicated that the three-deep arrangement was maintained even in the fully distended bladders of rats, rabbits, and dogs. In the human fetus, Hoyes, et al., (20) indicated that the three cell layers are developed by the fifth month.

The surface cells of the rat's bladder are irregularly cuboidal (22) and the external cell walls are keratonized (17, 18). A rigid segment of the cell wall extends down one-third the depth of the collapsed bladder's surface cell in rats, mice, rabbits, and dogs (31). Hicks (18) reported that keratin is in the form of tonofilaments and concluded that keratin formed the sub-surface fibrous network as an aid to the impermeability of the bladder. The mouse, rabbit, and human fetus also have a dense mat of fibers just below the thick, double membraned cell surface (11, 20, 44).

The other organelles of the surface cells show some minor dissimilarities between species. In the rat, the surface cells are attached to each other very firmly with zona adhaerens, occuludens, and desmosomes (17). The nucleus of the rat's surface cell is rounded with an irregular outline and small nucleoli (22). In contrast, the mouse has large nucleoli (44). In the mouse, the endoplasmic reticulum is in the form of tiny, well dispersed vesicles (44), while in the human fetus, the stacks are generally short, incompletely granular, and located at the periphery of glycogen deposits (20). In the rat, this organelle is usually located at the base of the surface cell (19). Hicks (19) described the rat Golgi in detail. He characterized it as having normal cisternae and associated small vesicles 500 to 900 A in diameter, some of which are free and others attached to the cisternae. The Golgi is located juxtanuclearly near the base of the cell. The cisternae's membranes vary in morphology, changing from the normal 75 A to a thickened 100 A unit membrane structure. This thickening of the membrane is not

complete, as only the luminal face is involved, and even then, not both leaflets at once.

Walker (44) described dense vesicles and granules of varying sizes in the mouse. The vesicles generally included remnants of membrane structure near their surface. In the rat, these membrane remnants formed a hexagonal geometric pattern (17). There are also empty vesicles randomly arranged in the rat's cytoplasm which are generally mixed with droplets of a lipid-like substance surrounded by limiting unit membranes (17). Leeson noted a small amount of dense material present in the rounded, supranuclearly located vesicles he described for the rat (22). Porter and Bonneville (30) demonstrated lysosomes in the transitional epithelium of the mouse, and Hicks (19) indicated that some of the vesicles previously described for the rat contained acid phosphatase. In another paper (17), he indicated that these vesicles were similar to lysosomes.

The structure of the intermediate cell layer of the rat contained the same cellular components previously described for the surface cells. However, less specialization was apparent as some structures described below were not present in their mature forms (22). The basal cell layer of the mouse and rat was the most unspecialized, having only the normal cellular components and lacking the specialized granules and vacuoles of the more superficial layers (22, 44).

The process of keratinization is studied most easily in the skin. Brody (4,5,6) and Bonneville (3) described keratin in the skin of guinea pigs, humans, and rats as being formed from a loose network of tonofilaments which mix with keratohyalin granules forming keratin. fibrils. Brody (5) also indicated that the tonofilaments came into close association with the keratohyalin granules and became denser and thicker. These keratin fibers were some 25 A thicker than the tonofilaments from which they were formed. This thickening was not a coating process, but rather a chemical alteration resulting in thicker structures. Brody (6) described the human keratohyalin granule as forming in the basal layers of the epithelium and migrating upwards with the cell during its maturation process.

Several types of cytoplasmic bodies have been described by various authors. In 1960, Walker (44) described a "whorl-like" structure in the intermediate cell layer of the rat. This structure was reported to have a core of small vesicles surrounded by concentric layers of membranes which apparently belonged to the agranular reticulum or Golgi (44). Hicks (17) reported a "bundle cell," a type of intermediate cell of the rat, which contained bundles of electron scattering material. These bundles had the appearance of 1,000 A by 70 A tubular crystallites. In some cells, these bundles were retained in membrane-bound vacuoles, some enclosed in incomplete membranes, and others were lying free in the cytoplasm. In the latter case, the surrounding cytoplasm was free of organelles, suggesting that the bundles were originally in a vacuole.

Hicks postulated that these differences were various developmental stages. Inclusions similar to those being described in this paper have been reported only in non-human primates.

Lucas, et al., (23) reported cytoplasmic inclusion bodies in the transitional epithelium of five to nine percent of Rhesus monkeys studied. He described these as being spherical to oval, acidophilic, and closely situated to the nucleus of the most superficial cell layer. These observations are confirmed by Burek, et al., (7). The size of these bodies were measured by both authors as being between three and ten microns in diameter.

Lucas, et al., (23) described a lace-like appearance of these inclusion bodies under the light microscope, and a tortuous, cohesive mass of fibers with the electron microscope. Burek, et al., (7) described them as whorled bundles of tightly packed filaments. In longitudinal orientation, the filaments consisted of paired beaded filaments measuring 50 A thick, separated from each other by 20 A, and from other pairs by 60 A. In cross section, he reported a hexagonal pattern that was composed of six fibrils (three pairs of filaments) 125 A in diameter and separated from adjacent angles by 60 A.

Burek, et al., (7) reported that the inclusions were not membrane bound, had a periodicity of subunits in longitudinal section, and occasionally possessed a continuity between the inclusion filaments and the tonofilaments. Based on histochemical studies, he reported that the inclusions were protein and possibly lipid in content. He

concluded that the inclusion bodies represented an aberrant development of tonofilaments. Lucas, et al., (23) also concluded that the inclusions were composed of tonofilaments. Neither author could demonstrate any pathological cause for the appearance of the inclusion bodies.

METHODS AND MATERIALS

Tissue for examination was collected from four M. fascicularis monkeys on different days. The tissue consisted of representative samples from the kidney pelvis, ureter, and urinary bladder. The animals were anesthesized with pentobarbitol. The tissue was surgically removed and divided into four parts. Parts I and II were used for electron microscopy studies. Part III was used for frozen tissue sectioning, and Part IV for paraffin embedding. Histochemical studies were performed on sections from Parts III and IV.

Part I was immediately placed in 2% osmium tetroxide dissolved in Millonig's phosphate buffer, minced into 1 mm cubes, and left for one hour. The samples were then transferred through three changes of buffer to rinse out excess osmium. The tissue was dehydrated in increasing concentrations of ethanol until it had undergone two 15-minute changes of 100% ethanol. The ethanol was decanted off and replaced with propylene oxide. Finally, a mixture of 50% propylene oxide and 50% Epon 812 (Ladd Research Industries, Burlington, Vermont) was used to displace the pure propylene oxide. The tissue samples were allowed to remain in the mixture overnight. The following morning, pure Epon 812 was used to replace the mixture.

Epon 812, a polymer, was mixed in a 50/50 v/v ratio from stock solutions of the A and B types of Epon 812. Type A consisted of 90 gm. dodecenyl

succinic anhydride and 80 gm. Epon 812. Type B was composed of 76 gm. nadic methyl anhydride in 100 gm Epon 812. To this mixture, a 2% volume of Tri (dimethyl amino methyl) phenol was added to act as the polymerization catalyst.

The tissue was left in the Epon 812 mixture under high vacuum until it was totally infiltrated. This end point was determined by the cessation of bubbles emerging from the tissue. The samples were then transferred to a fresh Epon 812 mixture in Beam capsules (Ernest F. Fullam, Schenctady, New York) and placed in 45° C and 60° C ovens until polymerization (curing) was complete.

Part II was treated in the same manner as Part I with the exception of the fixation used. Upon removal of the specimen from the animal and mincing of the tissue, the cubed specimens were placed in a 4% gluteraldehyde, cacodylate buffered solution for one hour, transferred to cacodylate buffer, and stored overnight. In the morning, it was placed in a 2 % solution of osmium tetroxide in cacodylate buffer for one hour. From this point, the tissue was processed identically to Part I.

Part III was quick frozen in liquid nitrogen at -196° C and stored in sealed plastic bags at -40° C. As needed, the tissue was sectioned on a CT International-Harris Cryostat at a thickness of six microns and mounted on clean glass slides.

Part IV was fixed in phosphate buffered formalin for ten days, processed through graded alcohols, xylene, and paraffin, and then embedded in paraffin blocks by standard procedures (35). Five micron sections were cut from these blocks using standard microtomy techniques. The sections were floated on a water bath containing gelatin before mounting on clean glass slides.

The cured blocks from Parts I and II were cut as 1 micron "thick" sections using glass knives and a Porter-Blum MT-2 Ultramicrotome. These sections were stained with toluidine blue and examined with a light microscope for areas of interest. The blocks were trimmed, leaving only these areas. "Thin" sections were then cut on a LK Reichert Om-U3 Ultra-Microtome using DuPont diamond knives. The sections were in the silver to silver-grey color range, correlating to a thickness of 500 to 700 A. The sections were then mounted on uncoated, 200 mesh copper grids.

These grids were post stained with uranyl acetate for 30 minutes, followed by a lead citrate stain for 90 seconds. The grids were then examined on a RCA EMU-3G Electron Microscope and micrographs were made with glass Kodak Electron Image Plates. Photographic enlargements were printed on Kodabromide and Kodak Polycontrast papers. Some high magnification and high resolution micrographs were made with a Hitachi HU-12A Electron Microscope.

The microscopes were calibrated with a 28,800 line/inch diffraction grating replica for each magnification setting. Negatives were exposed, and actual magnification values were calculated from measurements taken from the negatives. This information was, in turn, utilized in the calculations of the micrograph magnification. The extent of photographic enlargement was also taken into consideration in the final print magnification reported:

$$\text{Magnification} = \text{distance between lines on } \frac{\text{plate}}{\text{grating replica}}$$

$$\text{Micrograph magnification} = \text{magnification} \times \text{photograph enlargement}$$

The measurements of organelle size were made from the micrographs utilizing a calibrated hand lens. Calculations were then performed to obtain the actual object size:

$$\text{Object size} = \frac{\text{size on print in mm}}{\text{magnification}} \times 10^{7} \text{ A / mm}$$

The following stains and enzyme reactions were performed on frozen sections: hematoxylin-eosin (24), acid phosphatase (34), Nile blue (42), nucleal Feulgen reaction (35), acridine orange (37), methylene blue pH 3 with DNAase and RNAase digestion (36), oil red o (24), and periodic acid-Schiff reaction (29).

Paraffin embedded sections were stained with the following: hematoxylin-eosin (24), nucleal Feulgen reaction (35), methylene blue pH 3 with DNAase and RNAase digestion (36), ninhydrin-Schiff reaction (39), Millon reaction (41), Sakaguchi reaction (40), Nile blue (42), periodic

acid-Schiff reaction (29), Ziehl-Neelsen reaction (43), Ayoub-Shklar (2), and the DDD reaction (38). Each reaction was performed with a control section, kidney, and in the later stages of the study, monkey skin was used as a keratin control.

RESULTS

Eosinophilic inclusion bodies were seen in the surface layer of the transitional epithelium of the kidney pelvis, ureter, and the urinary bladder. When examined with the light microscope, these bodies were highly refractile and possessed an inner structure (plate 2). They were 1/2 to 1/3 the size of, and located close to, the nucleus. There were no discernable differences in the paraffin, frozen tissue, or Epon 812 sections. Development of the inclusion body appeared to progress from the basal and intermediate cell layers toward the surface. Plate 1 illustrates the straight forms in the lower cell layers and the mature inclusion bodies in the surface layer. This observation was supported by the electron microscopy examination of a large number of inclusion bodies.

Upon electron microscopic examination of the tissue, the inner structure of the mature inclusion body became apparent. They were seen to be composed of bundles of filaments arranged in a manner reminescent of a ball of twine. Certain portions of the same inclusion body were seen in cross and longitudinal section (plate 4). As with the light microscope, the mature inclusion bodies were 1/2 to 1/3 the size of the nucleus, and situated juxtanuclearly (plate 3). On higher magnification, the inclusion bodies appeared to encompass some of the numerous glycogen granules (plate 4) and a portion of a mitochondria (plate 5). The keratin fibers composing the mature inclusion body were 165 A in diameter.

The immature inclusion body (plate 5) which was found in the intermediate and surface cells, could be identified by the incomplete curling of the filament bundles. Some filament bundles still were in the juvenile straight form while others were beginning to coil. Numerous cytoplasmic constituants such as glycogen, which apparently were trapped in the coiling process, could be seen inside these coils. The immature inclusion bodies were very closely associated with the nucleus (plate 9). When the coiling was complete, the inclusion body was considered mature.

The mature inclusion body developed from an immature inclusion body and the latter, in turn, developed from straight form filament bundles (plate 8). These straight forms were composed of tightly packed filaments which were not membrane bound and were composed of fibers of the same diameter as the mature and immature inclusion bodies. The straight forms oriented perpendicularly to the bladder surface. The filaments were distinguished from tonofilaments by their thickness (25 A thicker than tonofilaments), their increased electron density, and their organization as tightly packed bundles of filaments (plate 8). In cross section (plate 14), the compactness of the filament bundles could be observed. Photographic enlargement of one of the bundles (plate 14) demonstrates the hollow tubule appearance of the filaments (plate 6). This characteristic was present in the mature inclusion body (plate 7) which shows the filaments cut in longitudinal section.

The measured wall thickness of the filaments in both longitudinal and cross section was 70 A. This value compared favorably with the expected wall thickness of a 165 A hollow tubule.

Many of the immature inclusion bodies and the straight forms of filament bundles were closely situated to membrane-bound organelles which resembled autophagosomes (plates 8, 9, 11, 13, 15, and 17). Many of these organelles had filaments inside their limiting membranes (plates 10, 12, 15, and 16). The diameter of these filaments averaged 87 A, which was smaller than the keratin filaments of the inclusion bodies. These autophagosomes were found in all three cell layers and could be associated with the filament development process in either a positive or negative way. The angles formed by the periodicity in these autophagosomes (plate 12) and the angles formed by the filament bundle in cross section (plate 14) were 47°, 63°, and 70°. It is conceivable that these autophagosomes were unrelated in the development process, as they are normal cellular organelles in most tissues.

Results for the histochemical procedures are listed in table 1. The following yielded positive reactions: Nile blue, Ziehl-Neelsen acid fast, Ayoub-Shklar (plate 1), Millon reaction, and the DDD reaction. Inconclusive results were obtained with the Sakaguchi reaction as both the control tissue, as well as the test tissue, gave negative reactions. Keratin controls gave similar results.

TABLE 1

HISTOCHEMICAL RESULTS

TEST	FROZEN TISSUE	PARAFFIN TISSUE	KERATIN CONTROL
Acid phosphatase	negative		
Nucleal Feulgen	negative	negative	
Acridine orange	negative		
Methylene blue, pH3			
DNAase	negative	negative	
RNAase	negative	negative	
Periodic acid-Schiff	positive	positive	positive
Nile blue	positive	positive	positive
Oil red o	negative	negative	negative
Hematoxylin-eosin	eosinophilic	eosinophilic	eosinophilic
Ninhydrin-Schiff		negative	negative
Millon		positive	positive
Sakaguchi		inconclusive	inconclusive
Ziehl-Neelsen acid fast		positive	positive
Ayoub-Shklar		positive	positive
DDD		positive	positive

DISCUSSION

The description of the inclusion bodies of the M. malatta (Rhesus) in previous reports (7, 23) and those in the M. fascicularis in this report are essentially identical. The appearance of the inclusion bodies under the electron microscope was also fundamentally indistinguishable. The histochemical reactions were similar although the interpretations differed.

The basis for the selection of the histochemical profile was governed by the desire to determine the composition of the inclusion bodies. One primary consideration was the possibility that the inclusions were of viral origin. To test this hypothesis, examinations for DNA and RNA were performed. The test used were the nucleal Feulgen reaction, acridine orange stain, and methylene blue reaction with enzyme digestion. All results were negative. The acid phosphatase enzyme reaction was selected to determine if the inclusion bodies were lysosomal. This test was also negative.

Based on positive acid fast stains, Burek, et al., (7) reported that the inclusion bodies were partially composed of a lipid. This conclusion of Burek, et al., (7) required tests which were designed to confirm the reported lipid content. These were the Nile blue reaction and the oil red o reaction. The Nile blue and acid fast reactions are used to identify lipid substances, but can indicate other materials and were positive. The oil red o reacts only with lipid and was negative. This indicated that there was no free lipid; that the positive acid fast and

Nile blue reactions were probably due to a protein, possibly keratin.

In an effort to confirm the presence of protein, several histochemical reactions were carried out. These were the Millon, Sakaguchi, and ninhydrin-Schiff reactions. The Millon reaction was positive, the Sakaguchi reaction was inconclusive due to technical problems, and the ninhydrin-Schiff reaction was negative which indicated that the protein had no reactive β-amino acid sites. As keratin is composed of protein, the positive Millon reaction is not surprising.

The possibility that the inclusion bodies contained a carbohydrate component was explored with the periodic acid-Schiff reaction which indicated that no carbohydrate was present in them. However, the cytoplasm was strongly reactive due to the large amount of glycogen present.

Analysis of the above test results seemed to indicate that keratin was possibly present. Other tests, not specific for keratin, but very indicative of its presence were then performed. They were the Ayoub-Shklar reaction and the DDD reaction (2, 8, 9, 18, 27). The Ayoub-Shklar reaction is an acid fuchsin and aniline blue-orange g stain that gives a positive reaction with keratin. While the stain was developed for the demonstration of keratin, it is not specific for it. The DDD reaction is specific for the S-S and S-H groups which are prevalent in keratin. Both reactions were positive, giving a total of five reactions that were indicative for keratin. These results can be interpreted as practical

proof that the inclusion bodies contain keratin.

It should be pointed out that keratin is merely a group of proteins, with similar properties, which are produced by epithelial cells (21). Its form should not be expected to be identical in different species or different tissues. Skin has its entire cell body transformed into the horney layer composed of keratin (4). Hair is also keratin (16), but hair is certainly different from skin. The papilla of the tongue has two different forms of keratin (13). It is not surprising then that the form that keratinization takes in the transitional epithelium is different that that occuring in other tissues and in other species.

The keratin filaments were observed in three stages of development: straight bundles of filaments, called straight forms, immature inclusion bodies which were characterized as being composed of a partially straight and partially curled filament bundle, and mature inclusion bodies which were totally composed of curled filament bundles. None were membrane bound and all were composed of 165 A filaments which were some 25 A thicker than the tonofilaments. This size relationship corresponds to that of keratinized filaments in skin (5).

In cross section, the filaments of the straight form (plate 8) and the mature form (plate 4) indicated that they were hollow tubes made up of subunits (plate 6). The fact that a keratin filament is hollow was well documented by Brody (4). However, the apparent subunit structure is merely an electronic optical illusion caused by a slight underfocus of

the microscope (28).

The reported sizes of the filaments composing the inclusion bodies were somewhat different from those obtained in this study. Lucas, et al., (23) reported a filament size of 120 A, Burek, et al., (7) reported 140 A, and I found a filament diameter of 165 A. These differences could be due to fixation techniques. Burek, et al., (7) used tissue that had been stored in formaldehyde, a very harsh fixative which could have caused the periodicity he described. Lucas, et al., (23) also stored his tissue in a fixative, gluteraldehyde, until he determined which samples to do ultrastructural studies on. These differences in filament sizes are not considered significant when the foregoing information is combined with the following considerations: The examinations were made on different microscopes which were probably calibrated differently, filament size measurements could have been made using different techniques, and fixative osmolarity values undoubtedly varied. A comparative analysis of the fine structure between the M. malatta and the M. fascicularis has not been reported, and such a study was beyond the scope of this investigation.

The reason that the keratin balls develop in primates is, at this point, purely speculative. It could be in a response to some stimulus in the urine or blood that causes the tissue to aberrantly produce a protective layer (18). This stimulating factor is not known, but in rats, keratinization is found associated with foreign body implantation, estrogen stimulation, and metaplasia induced by vitamin A deficient

diets (8, 9, 10).

The fact that keratin is formed in 100% of the M. fascicularis monkeys and in only a small percentage of other species could make M. fascicularis the experimental animal of choice in bladder keratinization studies.

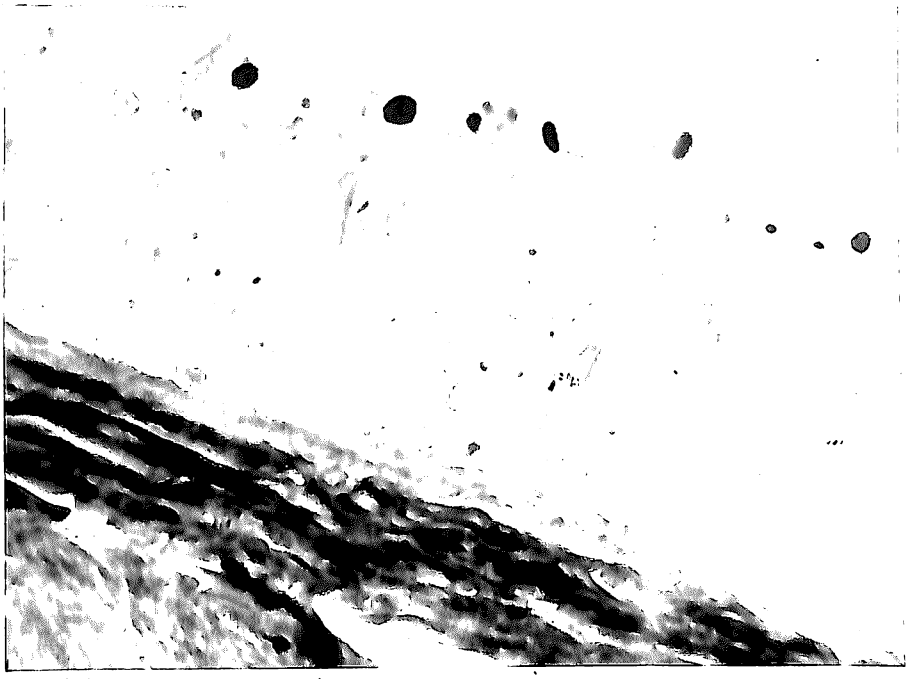

Plate 1 - A light micrograph of monkey urinary bladder epithelium with inclusion bodies (red) in the cell cytoplasm. Ayoub-Shklar stain for Keratin. X = 700.

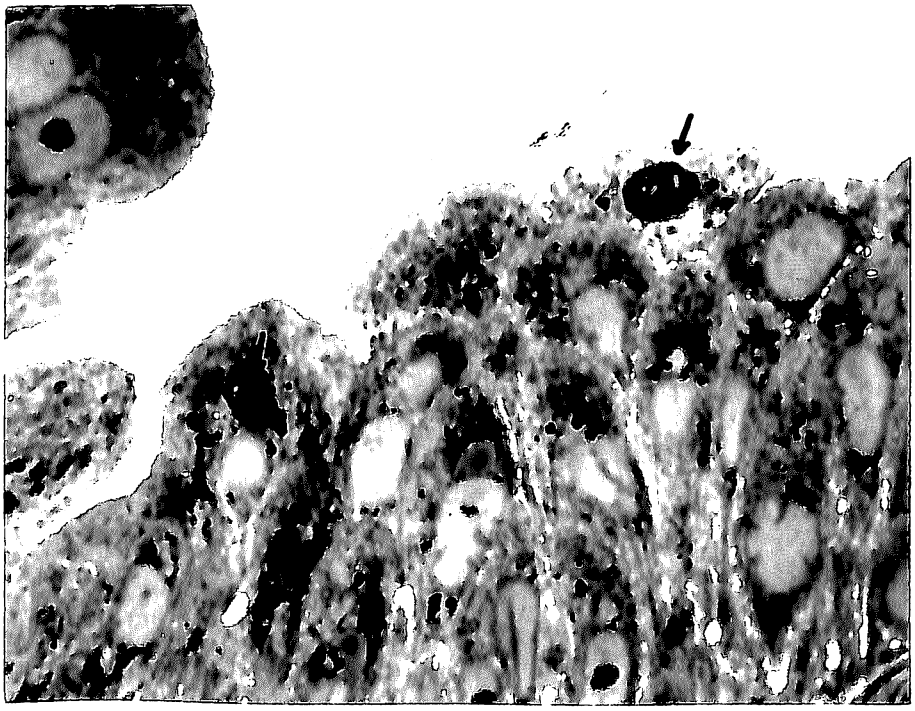

Plate 2 - A light micrograph of a 1 micron "thick" section of bladder epithelium embedded in Epon 812. Note the indication of an inner structure in the inclusion bodies (arrow). X = 1500.

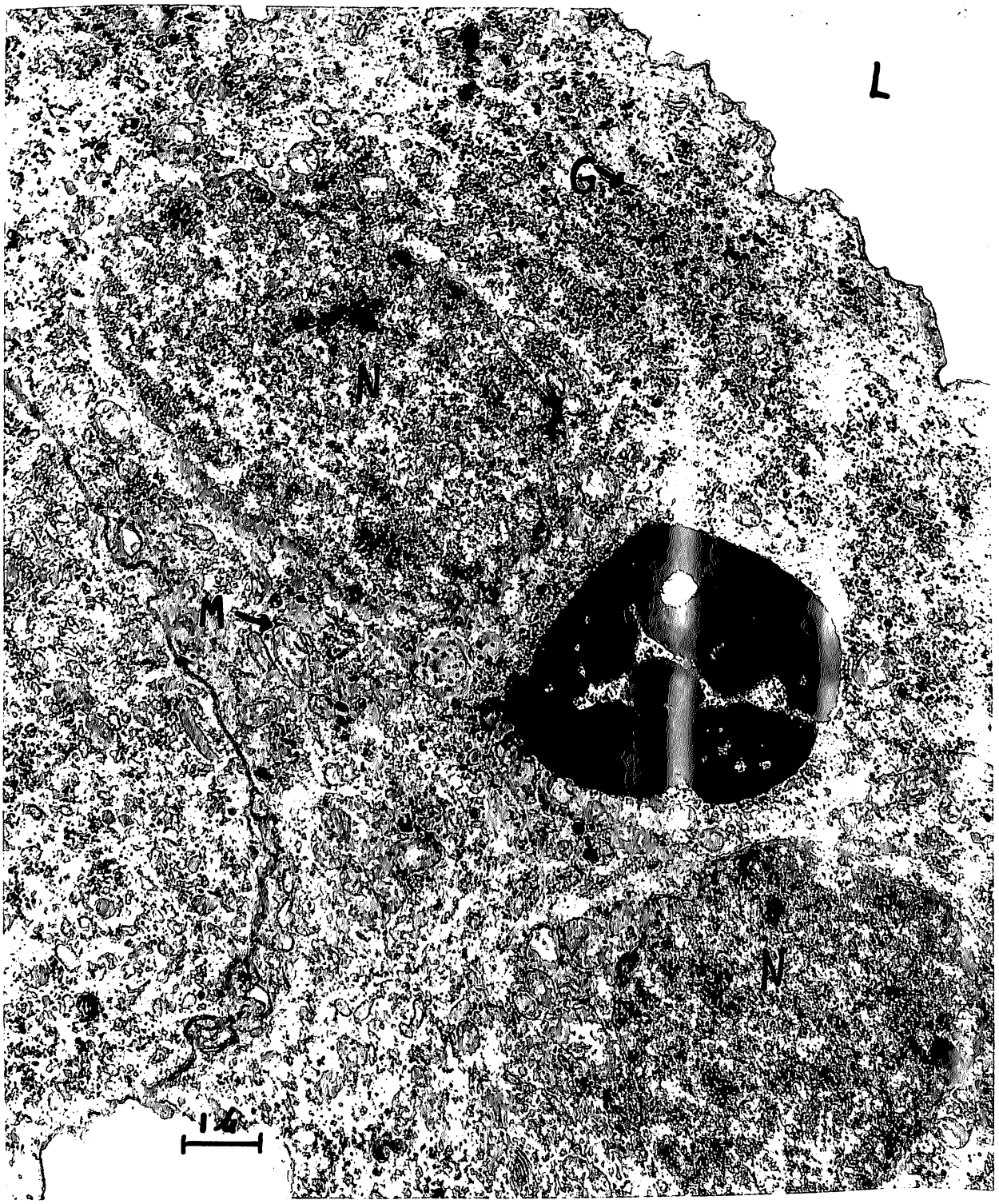

Plate 3 - A low-power electron micrograph of a mature inclusion body which was found only in the surface cells. N = nucleus, L = bladder lumen, G = glycogen, M = mitochondria. X = 10,275.

Plate 4 - A mature inclusion body with bundles of filaments sectioned longitudinally and in cross-section. Note the resemblance to a ball of twine. G = glycogen, SP = stain precipitant. X = 42,350.

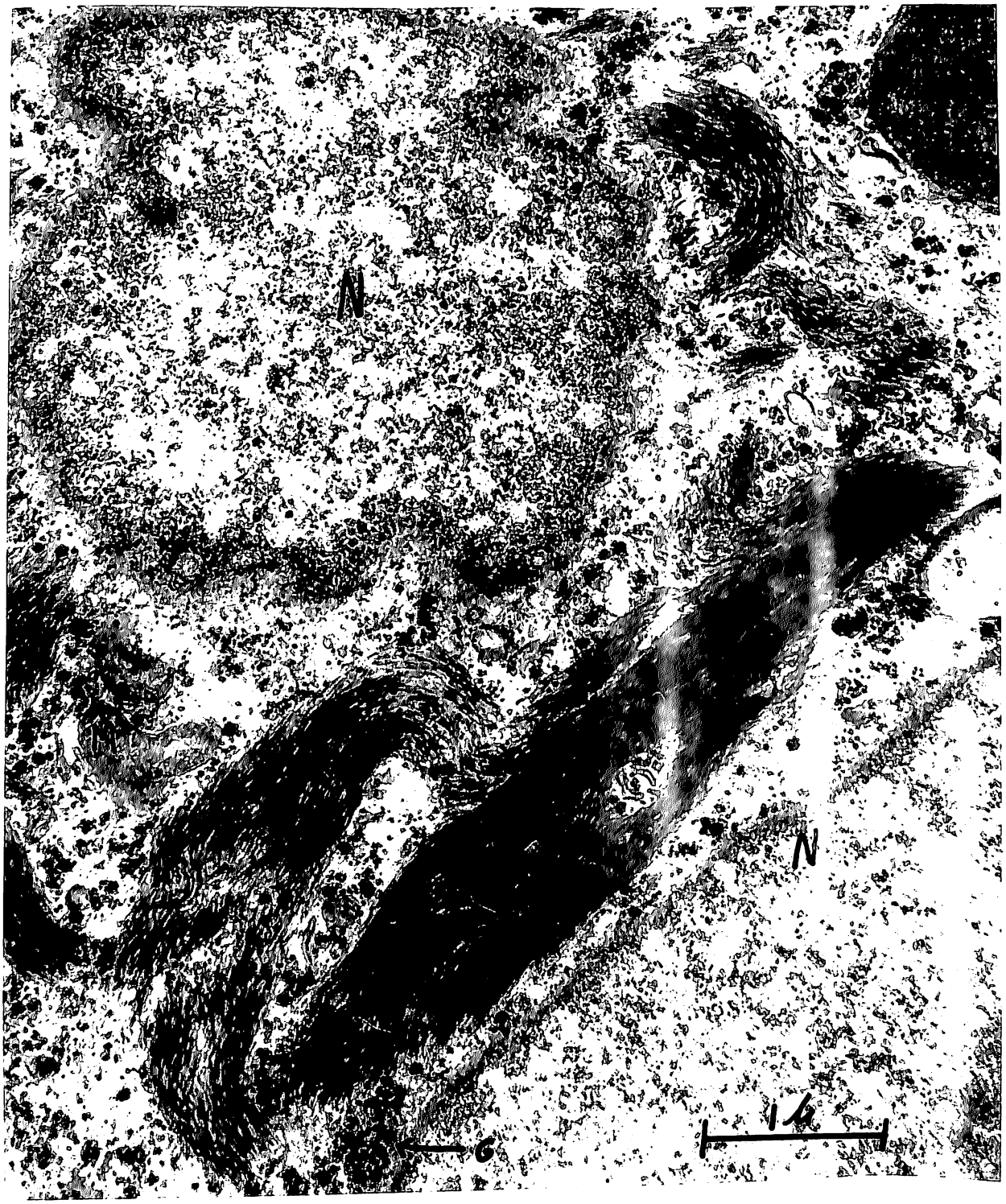

Plate 5 - An immature form of the inclusion body demonstrating the incompletely curled filament bundles which are characteristic of this stage of development. Note the close association with the nucleus (N).
A = autophagosome, M = mitochondria, G = glycogen. X = 27,500.

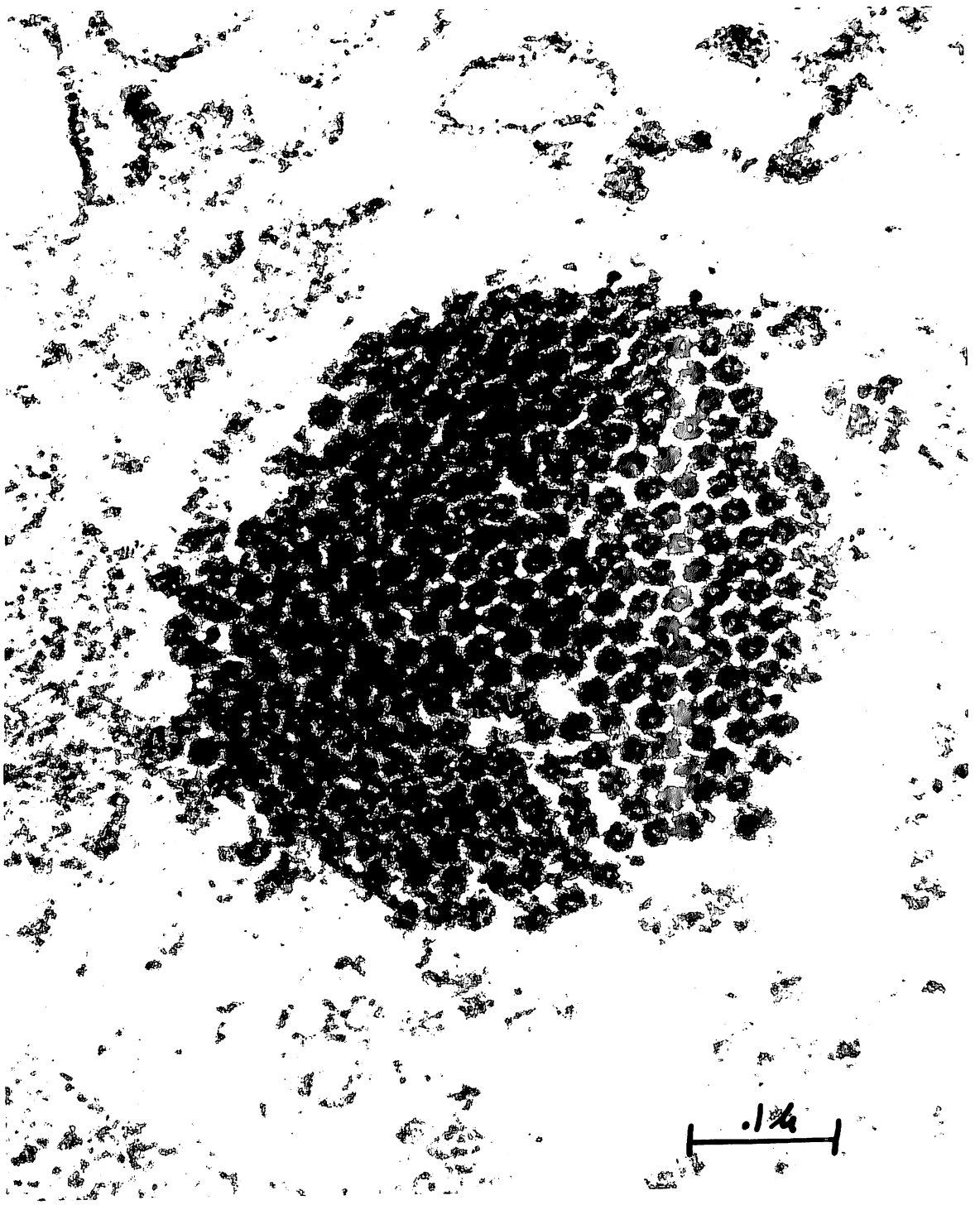

Plate 6 - A cross-section of the straight form of the keratin filament bundle demonstrating the hollow filaments characteristic of keratin filaments. The angles of the latticework are 70°, 63°, and 47°. X = 224,000.

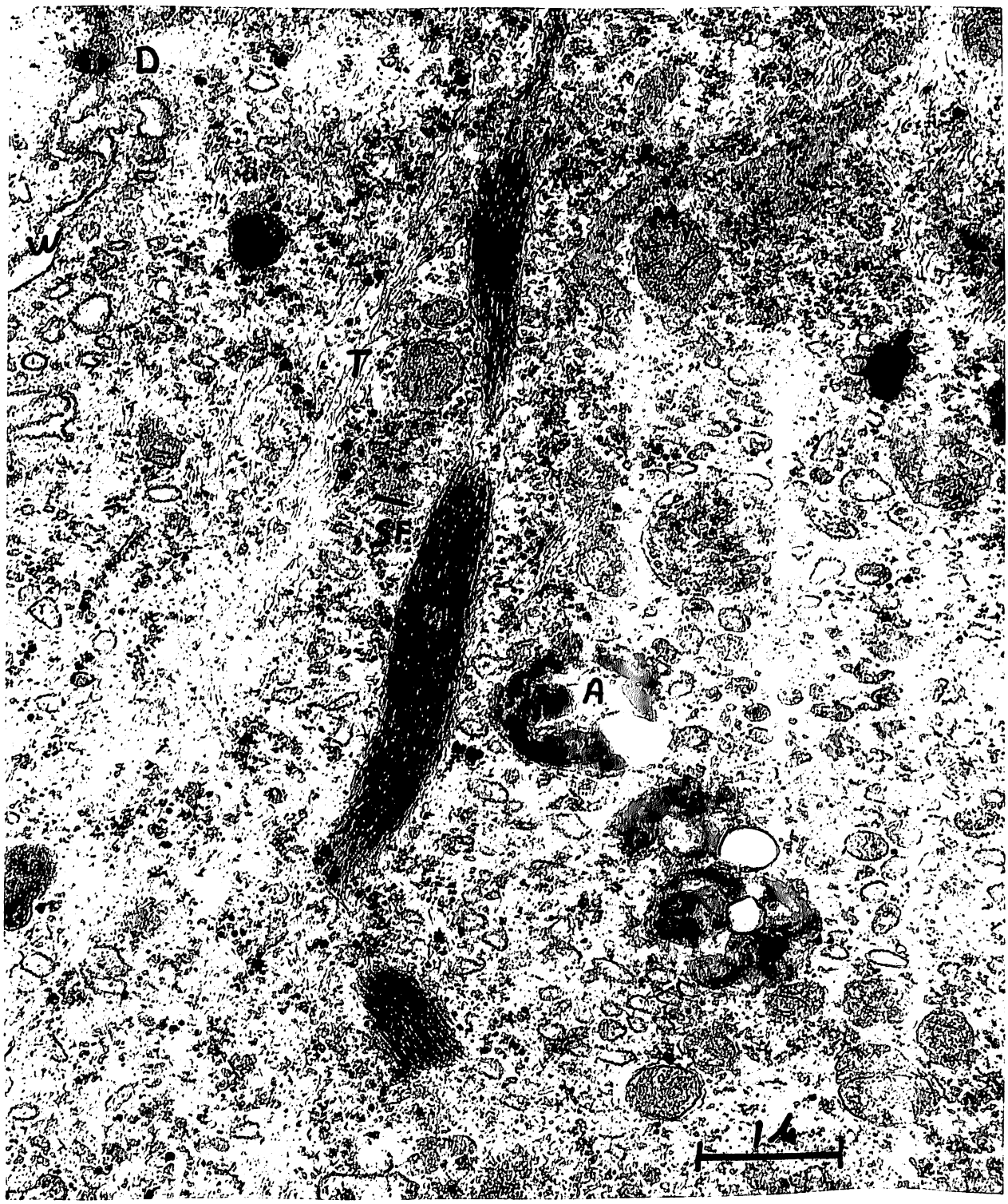

Plate 8 - The straight forms (SF) of the keratin filament bundles showing their distinct appearance when compared to the tonofilaments (T). A = autophagosomes, W = cell wall, D = desmosome, M = mitochondria. X = 21,175.

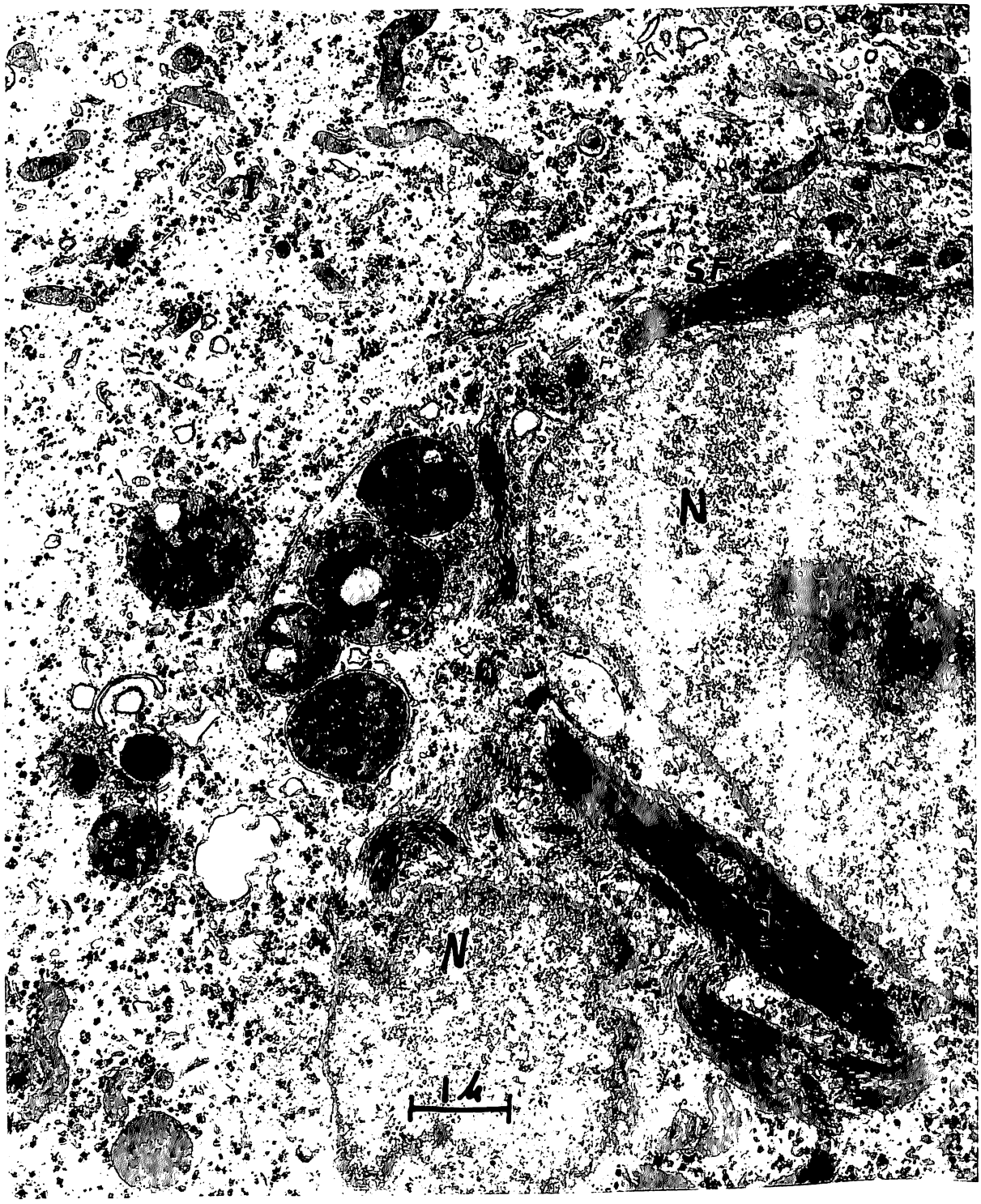

Plate 9 - The immature form (I) of the inclusion body and the straight form (SF) can be seen located in close proximity to the nucleus (N) and several possible autophagosomes (A). M = mitochondria. X = 15,000.

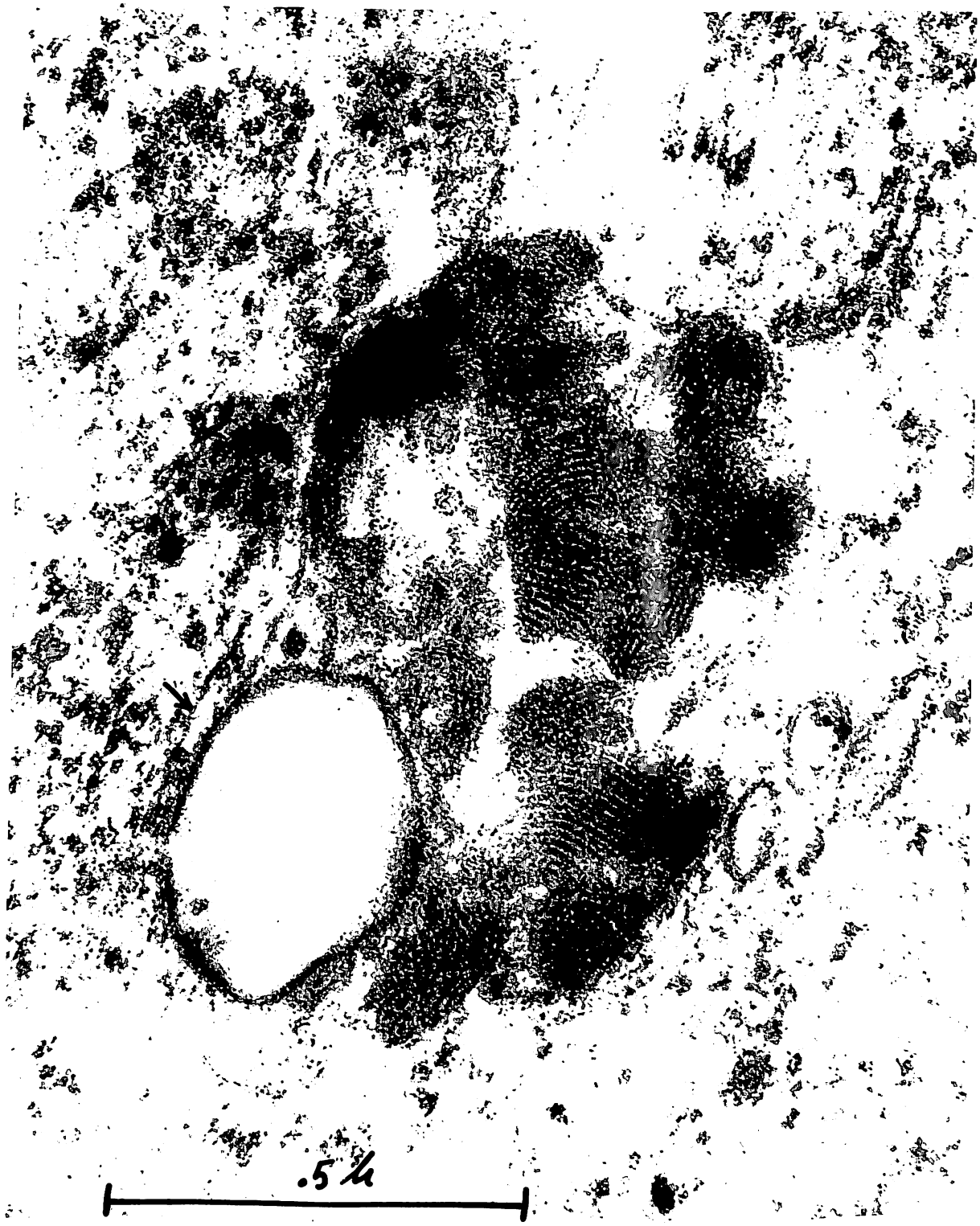

Plate 10 - A possible autophagosome with 85 A filaments inside its disintegrating membrane (arrow). X = 128,000.

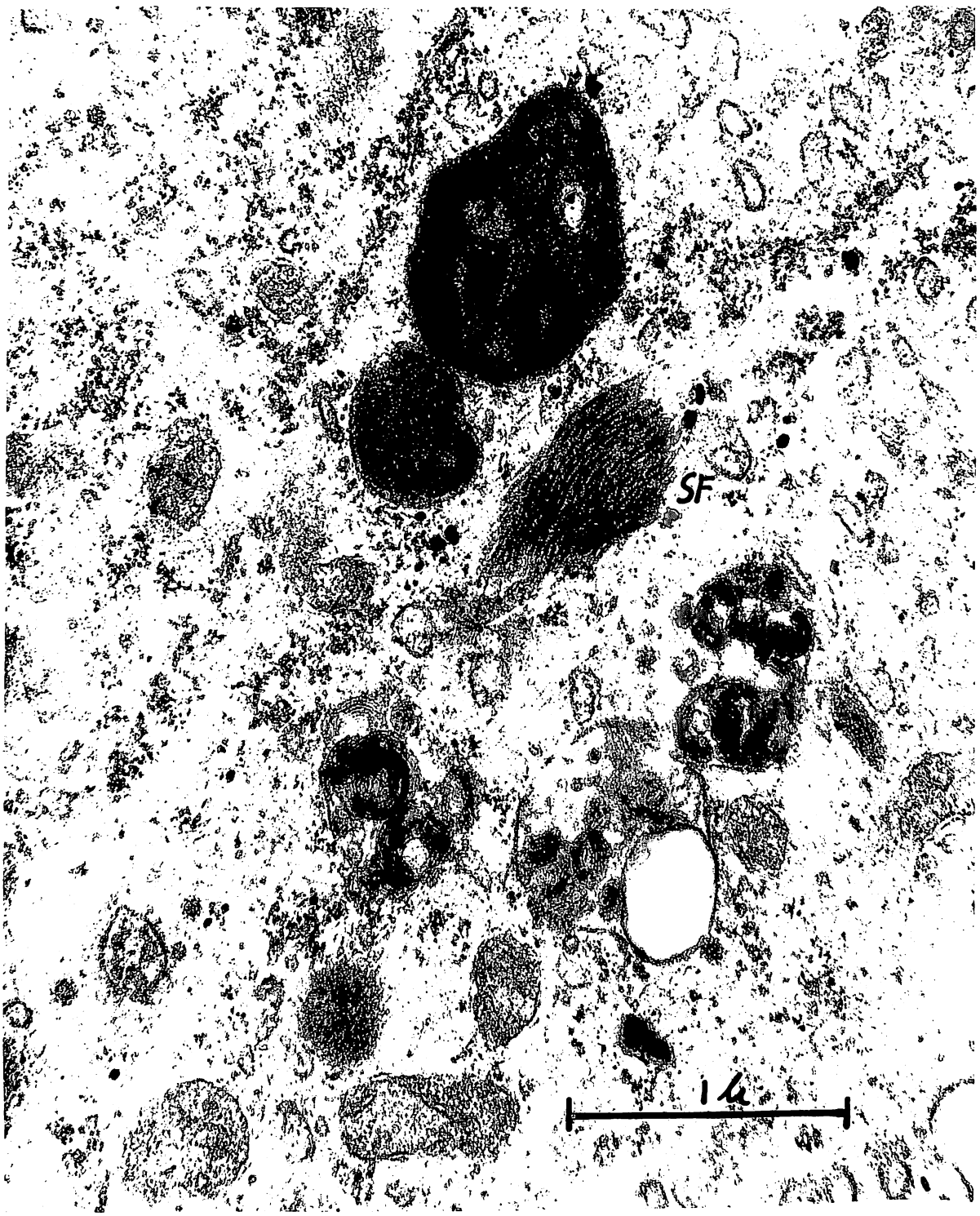

Plate 11 - A straight form (SF) of the keratin filaments can be seen closely situated (.2 microns) to several autophagosomes. X = 42,350.

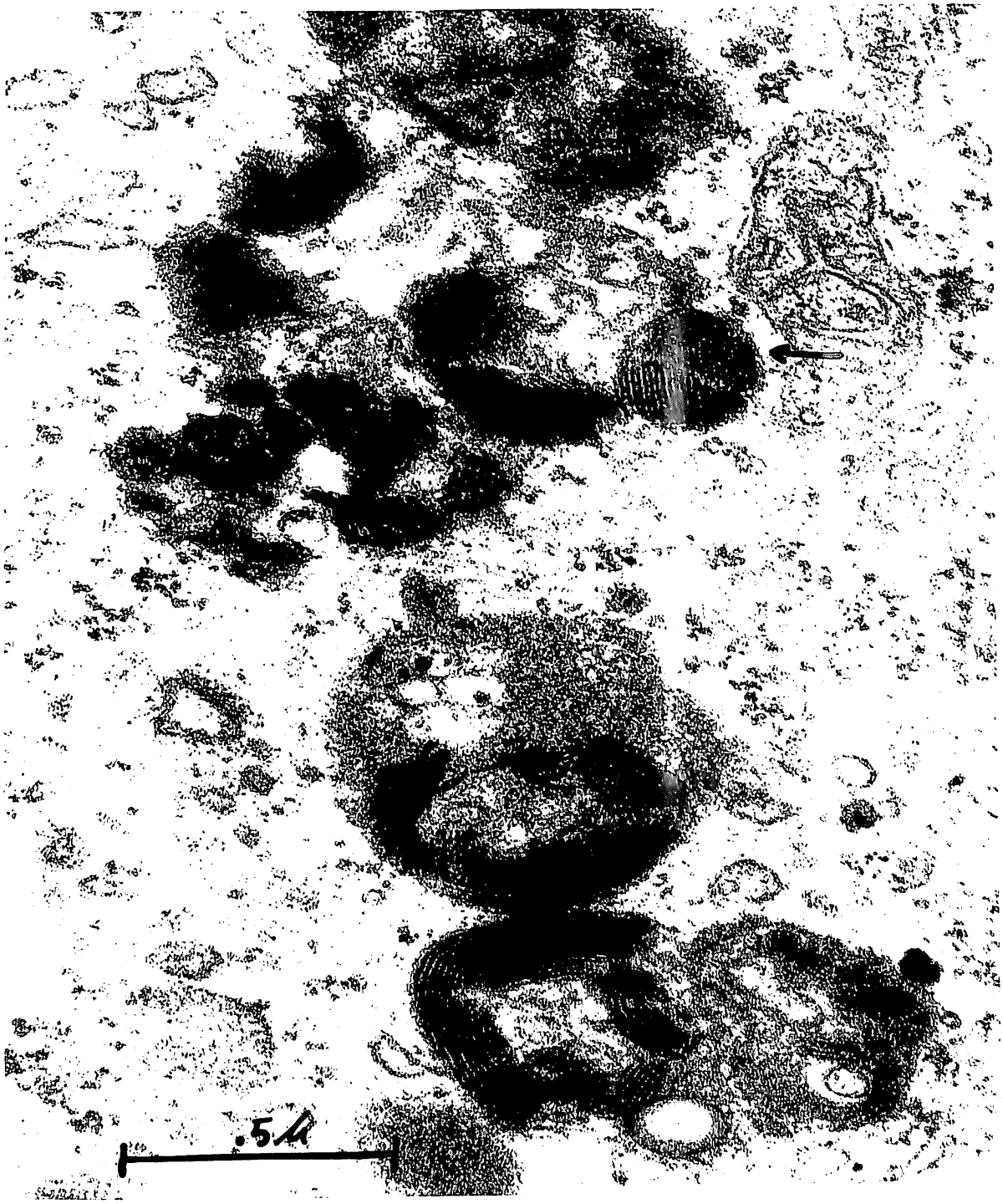

Plate 12 - Several autophagosomes with filaments in them can be seen. The arrow points out filaments whose periodicity is 87 A and whose matrix is 47°, 63°, and 70°. X = 80,000.

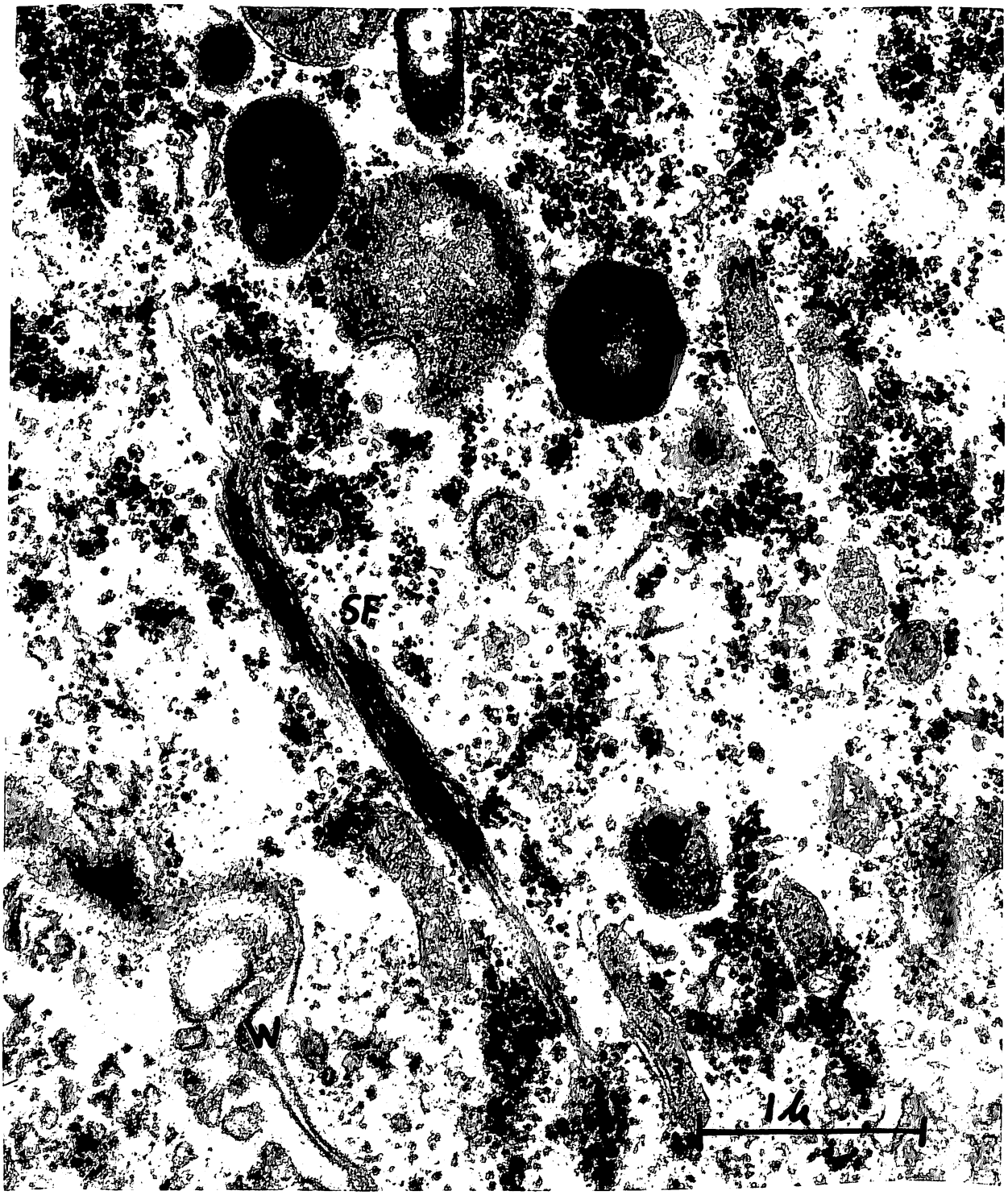

Plate 13 - Straight forms (SF) of keratin filament bundles in the intermediate cell layer. W = cell wall, M = mitochondria. X = 36,000.

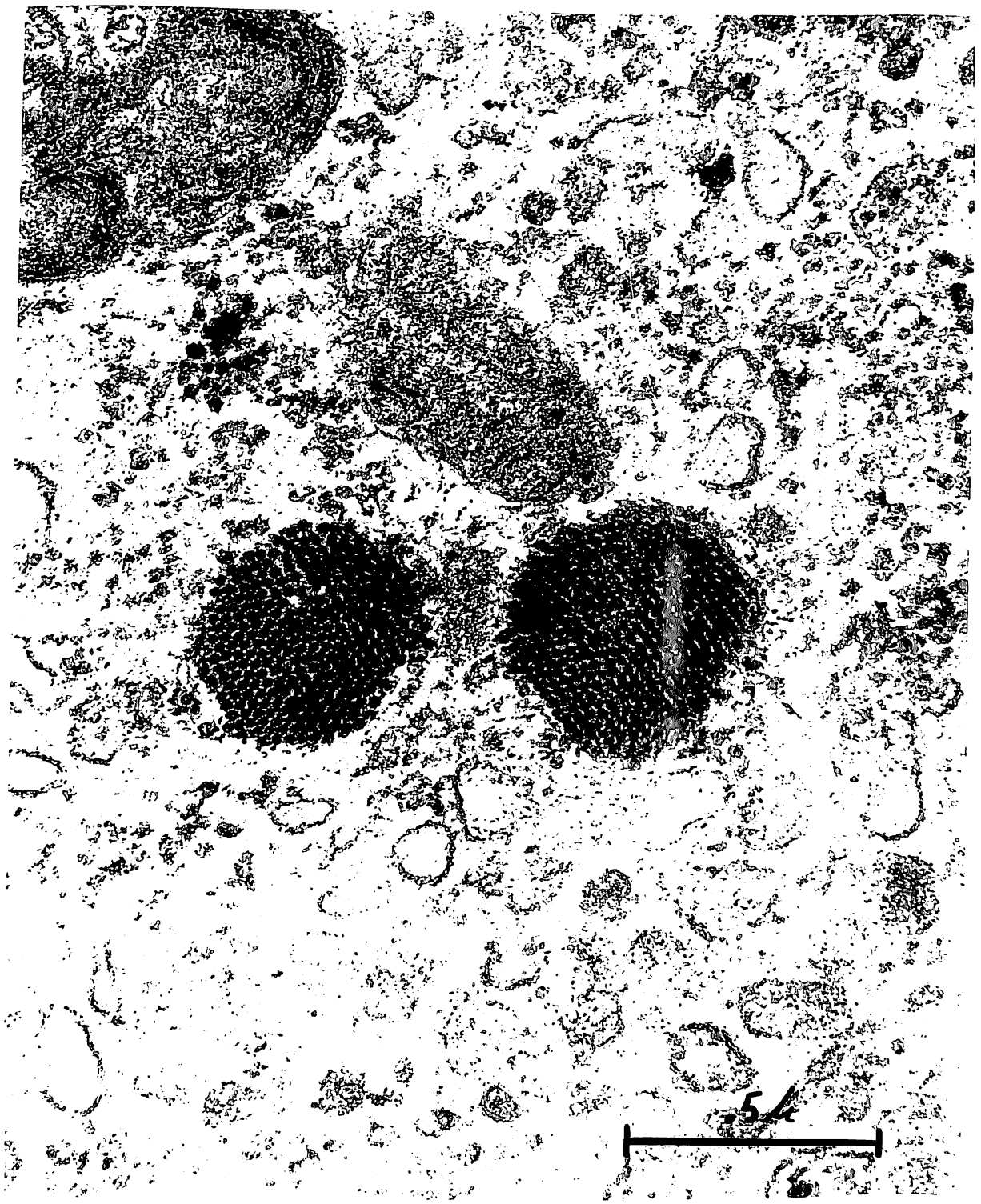

Plate 14 - A cross-section of two filament bundles of the straight form. This micrograph demonstrates that these are tightly packed with filaments and do not have a limiting membrane. X = 80,000.

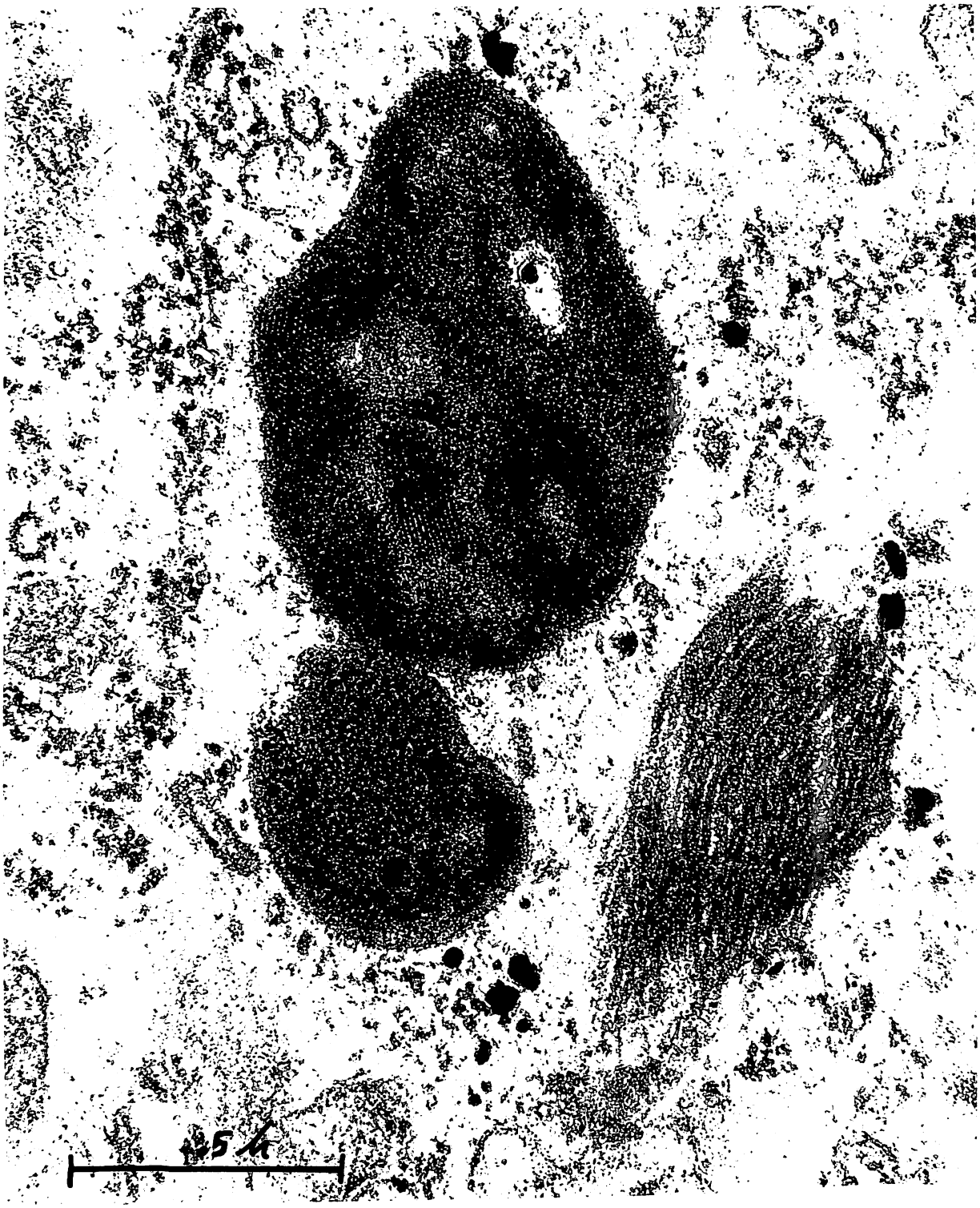

Plate 16 - A photographic enlargement of plate 11 which shows more detail of the keratin filament and autophagosome relationship. X = 84,700.

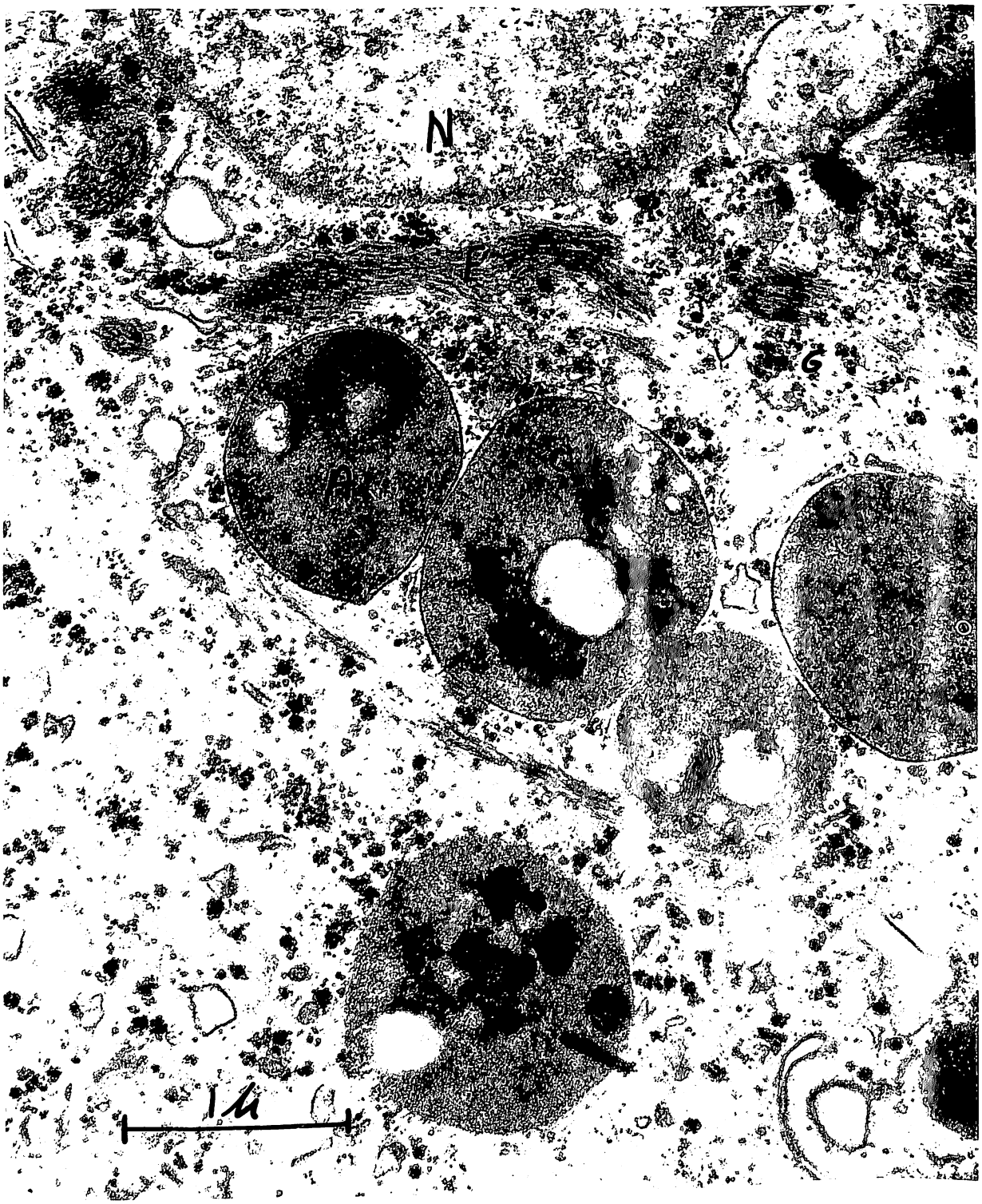

Plate 17 - This micrograph demonstrates the relationship of filament bundles (F) and autophagosomes (A) to the nucleus (N). G = glycogen. X = 36,000.

REFERENCES

1. Abdin, M. and Friedenstein, A. Y. Clinical Orthopaedics and Related Research, 82:182-194 (1972).

2. Ayoub, P. and Shklar, G. Oral Surgery, Medicine and Pathology, 16:580-581 (1963).

3. Bonneville, M. A. J. Anat., 123:147-164 (1968).

4. Brody, I. J. Ultrastruct. Res., 2:482-511 (1959).

5. Ibid., 3:84-104 (1959).

6. Ibid., 4:264-297 (1960).

7. Burek, J. D., Van Zwieten and Stookey, J. L. Vet. Path., 9:212-220 (1972)

8. Capurro, P. and Angrist, A. Archives of Path., 73:77-84 (1962).

9. Capurro, P., Angrist, A., Black, J., and Moumgis, B. Cancer Research 20:563-567 (1960).

10. Ibid., 20:568-572 (1960).

11. Chlapowski, F. J., Bonneville, M. and Staehelin, L. J. Cell Biol. 53:92-104 (1972).

12. DiFiore, M. S. H., An Atlas of Human Histology, 3rd ed. Lea & Febiger, Philadelphia, Pa., pp. 22, 180 (1967).

13. Farbman, A. I. J. Anat., 106:233-242 (1970).

14. Fawcett, D. W. An Atlas of Fine Structures - The Cell, W. B. Saunders co., Philadelphia, Pa., p 219 (1966).

15. Ham, A. W., Histology, 5th ed., J. B. Lippincott Co., Philadelphia, Pa., p 185 (1965).

16. Ibid., p 624.

17. Hicks, R. M. J. Cell Biol. 26:25-48 (1965).

18. Ibid., 28:21-31 (1966).

19. Ibid., 30:623-643 (1966).

20. Hoyes, A. D., Ramus, N. I., and Martin, B. G. H. J. Anat. 111:415-425 (1972).

21. Kligman, A. M. The Epidermis, Academic Press, New York, New York, pp 387-433 (1964).

22. Leeson, C. R. Acta. Anat. 48:297-315 (1962).

23. Lucas, J. A., Moser, J. H., and Scharden, J. L. Anat. Rec. 172:651-658 (1972).

24. Luna, L. G., ed Manual of Histologic Staining Methods of A.F.I.P., 3rd ed., McGraw-Hill Book Co., N.Y. (1968).

25. MacKenzie, W. F., USAFSAM/VSP, Brooks A.F.B., Texas 78235, Personal Communication.

26. Matoltsy, A. and Gedeon, J. Ultrastruc. Res. 29:438-458 (1969).

27. Matoltsy, A., Gedeon, J., and Matoltsy, M. N., Cell Biol. 47:593-603 (1970).

28. Millward, C. R., J. Vet. Res. 31:349-355 (1970).

29. Pearse, A. G. E., Histochemistry, Theoretical and Applied, 2nd ed., J & A Churchill Ltd., London p116 (1960).

30. Porter, K. R., Bonneville, M. A. Fine Structure of Cells and Tissues, 3rd ed., Lea & Febiger, Philadelphia, Pa., p 108 (1968).

31. Richter, W. R. and Moize, S. M. J. Ultrastruc. Res. 9:1-9 (1963).

32. Roberts, J. A., and Seibold, H. R. Folia Primatol, 14:59-69 (1971).

33. Rogers, G. E. In The Epidermis, Academic Press, New York, N.Y., p 189-197 (1964).

34. Sigma Technical Bulletin #85, Sigma Chemical Co., St. Louis, Mo. (1971).

35. Thompson, S. W., Selected Histochemical and Histopathological Methods, Charles C. Thomas, Springfield, Ill. p 261 (1966).

36. Ibid., p 267.

37. Ibid., p 269.

38. Ibid., p 304.

39. Ibid., p 310.

40. Ibid., p 314.

41. Ibid., P 314.

42. Ibid., p 334.

43. Ibid., p 1025.

44. Walker, B. E. J. Vet. Res. 3:345-361 (1960).

ACKNOWLEDGMENTS

The author wishes to express his gratitude to the United States Air Force School of Aerospace Medicine, Brooks Air Force Base, Texas for its generous assistance in the completion of this research project. In particular, the equipment, supplies, and advice provided by the Veterinary Pathology Branch and its chief, Lieutenant Colonel William F. MacKenzie, were invaluable. My deepest appreciation to my colleagues in the Radiation Biology Branch for their critical discussions and advice. The consultations with Charles D. Montgomery, Carl R. Nielsen, and Yolanda L. Salmon were particularly helpful.

The assistance of the Armed Forces Institute of Pathology in the performance of the DDD reaction was indispensable.

The secretarial tasks performed by my loving wife, Sally, were most appreciated.

Alan B. Weckerling